effect of these high acid numbers on the ZSM-5 performance is unknown.

## G. Slurry Reactor Hydrodynamic Studies

### 1. Bubble-Column Gas Holdup

The bubble-column reactor of the BSU was designed to gather gas holdup data using a differential pressure (DP) measuring system, and catalyst concentration data using a slurry sampling system (see Section IV.C for detailed description of these systems). Such data are essential for analyzing the performance of the reactor, for providing essential parameters for a slurry reactor mathematical model, and for characterizing factors in scale-up of the slurry reactor.

During Run CT-256-1, the DP measuring system was inoperative due to plugging of the DP nozzles and lines. However, the average gas holdups were estimated by accounting for the quantity of the reactor-wax between the view-ports along the slurry reactor and the feed-gas distributor. These estimations were done at the beginning and the end of the run. In Run CT-256-3, after modifications, the DP measuring system performed well and gas holdup profiles were estimated. The highlights of these experiments are:

- In Run CT-256-1, the initial gas holdup was very high (about 63 vol % at 2.2 cm/s feed-gas superficial velocity) probably due to the initial reactor-medium used. At the end of the run the gas holdup was 29% at 1.8 cm/s.
- There were no significant changes in gas holdup during the major part of Run CT-256-3.
- The average gas holdup increases with decreasing slurry level. This is consistent with the existence of a three-zone gas holdup profile first postulated by Langemann and Koelbel (1967).
- At low gas velocities, a hysteresis phenomena was observed, i.e., increasing the velocity did not instantly increase the gas holdup. This may have been due to catalyst settling at the low velocity, and difficulty to reentrain the catalyst at the higher velocity.
- The measured gas holdups were consistently higher than those reported by Deckwer, et al, (1980).

At the beginning of Run CT-256-1, a given quantity of the slurry was loaded into the first-stage bubble column reactor. By observing the slurry level at the viewport at 762 cm height, a gas holdup of 63 vol % at 2.2 cm/s superficial gas velocity was estimated. Such a high gas holdup was unexpected and greatly limited the initial loading of the F-T catalyst during the run. At the end of the run, slurry was withdrawn in stages by observing the slurry levels at the three viewports along the reactor. The quantities of the slurry withdrawn between viewports were measured and used to estimate the average gas holdups:

| DOS | $u_{gm}$ cm/s | $w_c$ wt % | L cm | Avg. $\epsilon_g$, Vol % This Study | Avg. $\epsilon_g$, Vol % Deckwer, et al. (1982b) |
|---|---|---|---|---|---|
| 0.0 | 2.2 | 6.7 | 762 | 63 | 13 |
| 60.8 | 1.8 | 2.5 | 762 | 29 | 10 |
| 61.1 | 2.2 | 2.5 | 610 | 32 | 13 |
| 61.1 | 2.2 | 2.6 | 305 | 42 | 13 |

By comparing the average gas holdups of 762 cm column height at both the beginning and the end of the run, a drastic reduction in the gas holdup was observed. This was probably due to changing slurry medium during the run. The startup reactor-wax was very different from the equilibrium reactor-wax later established in the reactor (see Section VI.B for detailed description of startup wax used). The gas holdups at 762, 610 and 305 cm height estimated at the end of the run show that the average gas holdup increases when the column height decreases. This observation is consistent with that of Langemann and Koelbel (1967) in a non-reacting, cold-flow system. Similar results were also observed in a 2.5 cm ID hot-flow, non-reacting column, as reported later in Section VIII.E. A description of the existence of a three-zone gas holdup profile, first postulated by Langemann and Koelbel (1967) to explain this phenomena is also included in that Section. The above table also includes the gas holdups estimated from the correlation $\epsilon_g = 0.053\ (u_g)^{1.1}$ developed by Deckwer, et al. (1980). These estimated values are consistently below the corresponding experimental values.

Table 25 summarizes overall gas holdups taken from different times on-stream of Run CT-256-3. It can be seen from this table that the holdup did not change very much over the first seventy-five days on-stream. However, the data from seventy-nine to eighty-one DOS show a hysteresis effect of the gas holdup. That is, after the velocity was dropped to 1.1 cm/s, the gas holdup did not respond instantly with raising the velocity. This may have been due to catalyst settling at the low velocity as described earlier, and difficulty in re-entraining

Table 25

Summary of Estimated Gas Holdup from DP-Cell Data

(Run CT-256-3)

| | | | | | |
|---|---|---|---|---|---|
| DOS | 9.2 | 75.5 | 78.6 | 78.8 | 80.8 |
| $u_g^i$, cm/s | 3.9 | 2.6 | 1.1 | 2.6 | 2.6 |
| T, °C | 260 | 267 | 260-267 | 260-267 | 267 |
| P, MPa | 1.48 | 2.51 | 2.51 | 2.51 | 2.51 |
| $w_c$, Wt % | 14.3 | 13.9 | 11.7 | 12.0 | 12.0 |
| $\epsilon_g$, Vol % | 26.6 | 19.7 | 6.8 | 9.3 | 19.8 |

the catalyst at the higher velocity. Figure 33 illustrates the typical gas holdup profiles along the bubble-column reactor in Run CT-256-3. This profile is similar to that reported by Langemann and Koelbel (1967) in cold-flow bubble-columns.

The gas holdup near the top of the column is high, due to the fact that the bubbles have to disengage from the slurry, i.e., an end effect. At the bottom of the column there is a short zone where the gas holdup changes dynamically with distance. This arises from the bubble dispersion, formation, and coalescence. After that the holdup decreases, probably due to the fact that the gas volume contracts as the reaction proceeds. Two separate profiles show that the gas holdup is similar at the beginning and the end of the run, with absolute differences due to the change in the gas velocity.

2. Bubble-Column Catalyst Settling

Uniform catalyst distribution in bubble-column reactors is important for obtaining effective use of the catalyst and for maintaining a uniform slurry temperature. During operation of the BSU, catalyst concentration profiles were occasionally obtained by taking slurry samples from several fixed locations of the bubble-column reactor and then by burning off the wax from the samples. The solids concentration profiles for different days on-stream of Run CT-256-3 are plotted in semi-log fashion in Figure 34 corresponding to different gas velocities. The straight lines shown by this plot indicates that the trend of the catalyst concentration profile follows very well the established particle settling mathematical model in bubble-columns (Kato, et al., 1972). Highlights of this figure are:

- Increased velocity decreases the catalyst settling, so a flatter profile is achieved.

- The profile is steeper during the hydrodynamics upset at eighty-two DOS, indicating increased catalyst settling. The profile after the upset is slightly flatter.

No meaningful catalyst concentration profile data are available between ten and eighty-two DOS. It also is not clear if the steeper concentration profile at the end of the run could be completely attributed to lower gas velocity.

A "hydrodynamic upset" of the slurry reactor occurred at eighty-two DOS, probably due to catalyst settling, resulting in a low $H_2$+CO conversion and a 5°C lower temperature at the upper portion of the reactor. The upset disappeared after eight hours of high gas velocity operation, but reappeared after the velocity was lowered (see Section VI.D for description of Run CT-256-3).

# FIGURE 33

## SLURRY FISCHER-TROPSCH BUBBLE-COLUMN GAS HOLDUP PROFILES

## (Run CT-256-3)

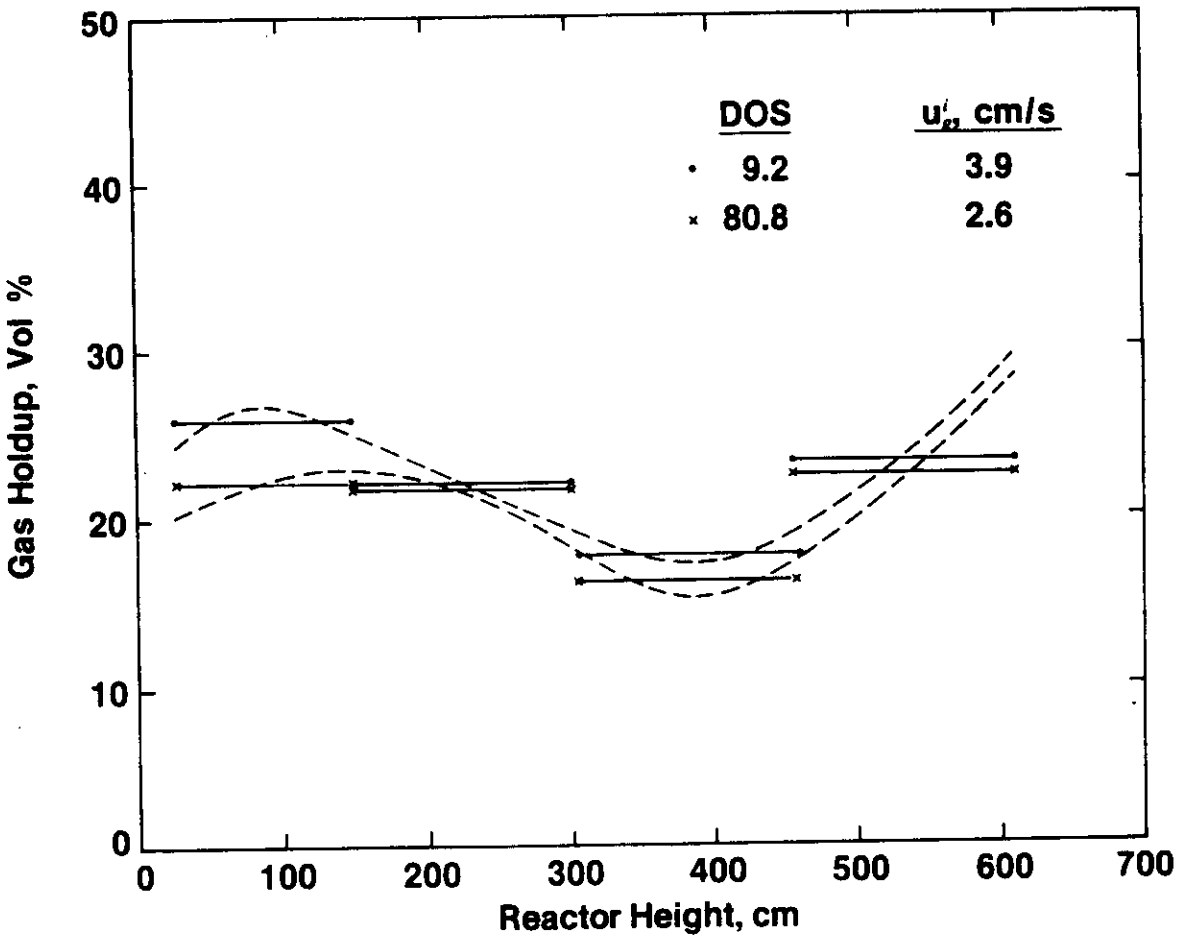

# FIGURE 34

## SLURRY FISCHER-TROPSCH BUBBLE-COLUMN CATALYST CONCENTRATION PROFILES

## (Run CT-256-3)

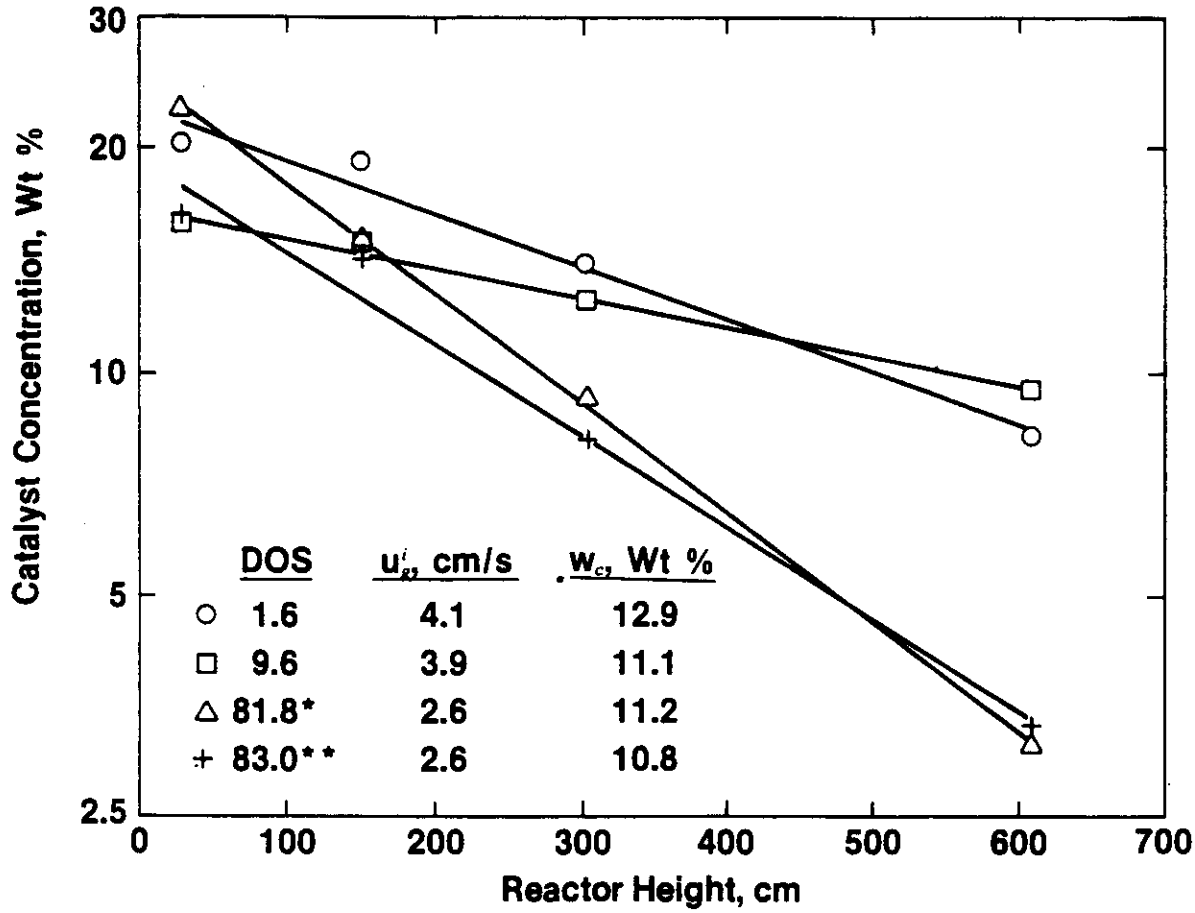


*During hydrodynamic upset

**After hydrodynamic upset was corrected

## VII. Fischer-Tropsch Bubble-Column Reactor Mathematical Models and Their Applications

### A. Introduction

The design and operation of the second-stage ZSM-5 fixed-bed reactor are rather straightforward. On the other hand, the slurry Fischer-Tropsch reactor is unconventional and involves complicated transport phenomena. A realistic mathematical model of such a system would be extremely useful in aiding the pilot plant reactor design and the data interpretation.

There were several published mathematical models of Fischer-Tropsch bubble-column reactors, e.g., Deckwer, et al. (1981a and 1982b), Satterfield and Huff (1980), and Stern, et al. (1983). Each of these models accounted for certain features of the Fischer-Tropsch bubble-column reactor, but none were sufficiently complete to provide good reactor design and data interpretation. For example, Deckwer et al. (1981a and 1982b) used single component ($H_2$) models and simple first-order kinetics for the F-T rection; Satterfield and Huff (1980) simplified the model further by assuming no volume contraction by the F-T reaction; Stern, et al. (1983), although using a multi-component ($H_2$, $CO$, $CO_2$, $H_2O$) model, did not consider the interaction between the F-T and the water-gas shift reactions and used an unrealistic expression for the volume contraction due to the F-T reaction.

In this chapter, some simple, single-component ($H_2$) F-T reactor mathematical models were developed first to evaluate the F-T bubble-column performance and to determine the conditions for optimal utilization of the reactor volume. An improved multi-component mathematical model was then developed. This sophisticated model takes into account the existence of both the F-T and the water-gas shift reactions, the non-linear kinetic expressions for both reactions, and multi-component ($H_2$, $CO$, $CO_2$ and $H_2O$) transport phenomena.

### B. Transport Phenomena in Slurry Fischer-Tropsch Reactors

In a slurry F-T reactor, the following transport and kinetic steps occur:

1. Transfer of the reactants from the bulk gas phase to the gas-liquid interface.

2. Transfer of the reactants from the gas-liquid interface to the bulk liquid phase.

3. Mixing and diffusion of the reactants in the bulk liquid phase.

4. Transfer of the reactants to the external surface of the catalyst particles.

5. Diffusion of the reactants inside the catalyst pores to the catalyst active sites.

6. Conversion of the reactants to products at the active sites.

7. Diffusion of reaction products from the active sites to the catalyst particle surface.

8. Transfer of the products from the catalyst to the bulk liquid.

9. Transfer of the products from the bulk liquid to the gas-liquid interface.

10. Transfer of the products from the gas-liquid interface to the bulk gas.

The first six transport and kinetic steps contribute the resistances to transfer the reactants from the bulk gas to the catalyst and their conversion to products. Steps 7-10 contribute the resistances to transfer the products from the catalyst to the bulk gas. Of these, steps 5 and 7, the internal diffusion resistance, are negligible due to the very small size of the catalyst particles, usually $\leq 50\mu m$.

In order to determine the relative resistance contributed by each transport step, it is sufficient to evaluate the transport of $H_2$ (Steps 1-4). Figure 35 shows a schematic concentration profile, and definitions and typical values of those resistances. The values of the parameters used in calculating the typical values of those resistances are summarized in Table 26.

The largest resistance among all the steps is the kinetic resistance. However, the resistance attributed to the diffusion of $H_2$ from the gas-liquid interface to the bulk liquid is also important. Other resistances are negligible. Hence, only Steps 2, 6, and 9 are considered in constructing mathematical models.

FIGURE 35

MASS-TRANSFER RESISTANCES IN A GAS-LIQUID-SOLID SYSTEM

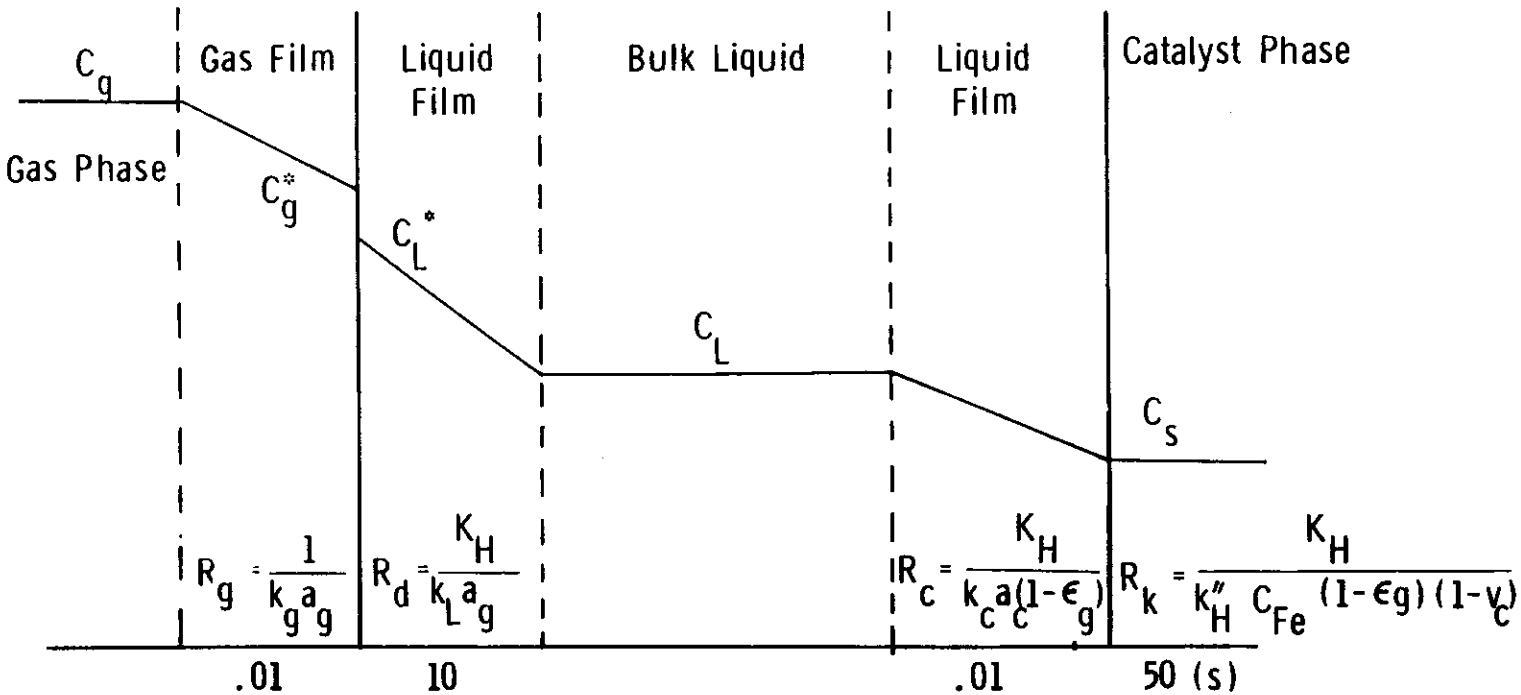

Table 26

Parameters Used in Single-Component
F-T Slurry Reactor Mathematical Model Calculations

| | |
|---|---|
| $T = 265°C$ (509°F) | $C_c = 0.1$ g/cm$^3$ (6.2 lb/ft$^3$) |
| $P = 1.38$ MPa (200 psia) | $f = 0.7$ |
| $u_g^i = 4$ cm/s (0.13 ft/s) | $U = 1/1.55$ |
| $d_c = 2.5$ $\mu$m | $d_B = 0.7$ mm |
| $\epsilon_g = .243$ | $k''_H = 1.1$ cm$^3$ liquid/s-gFe |
| $K_H = 4.4$ | $k_L = .013$ cm/s |
| $k_c = .39$ cm/s | $k_g = 3.43$ cm/s |
| $\rho_c = 2.6$ g/cm$^3$ | |

## C. Bubble-Column Mathematical Models

### 1. Single-Component ($H_2$) Models

Single-component mathematical models were developed to assist in design and operation of the bench-scale bubble-column reactor. The major assumptions of these simple models are:

- Mass transfer resistance to diffusion at the liquid side of the gas-liquid interface.
- Single Fischer-Tropsch reaction

  $CO + U\ H_2 \text{-----} > \text{Products}$

  with first order rate in $H_2$

  $r_H = k_H''\ C_{HL}$ (Mol $H_2$/gFe-s)
- Constant $H_2/CO$ usage ratio U
- Molar contraction due to synthesis reaction is a linear function of synthesis gas conversion
- Constant bubble-size and gas holdup
- Steady-state isothermal and isobaric operation
- Plug flow gas

The material balance equations are:

Gas Phase

$$d(u_g\ C_{Hg})/dz = k_{LH}\ a_g\ (C_{HL} - C_{Hg}/K_H) \qquad (5)$$

Convection in Gas Phase — Diffusion from Gas-Liquid Interface to Liquid

Liquid Phase

Non-Mixed (NM):

$$k_{LH}\ a_g\ (C_{HL} - C_{Hg}/K_H) = -k_H''\ C_{Fe}(1-v_c)(1-\epsilon_g)C_{HL}C_c/C_{ca} \qquad (6)$$

Diffusion from Gas-Liquid Interface to Liquid — Kinetic Dissipation at Catalyst Surface

Perfectly Mixed (PM):

$$\int_0^L k_{LH}\, a_g\, (C_{HL}-C_{Hg}/K_H)\, dz = -k_H''\, C_{Fe}(1-v_c)(1-\epsilon_g)\, C_{HL}L \qquad (7)$$

Diffusion from Gas-Liquid Interface to Liquid — Kinetic Dissipation at Catalyst Surface

Axially dispersed (AD):

$$E_L\,(1-\epsilon_g)\,(1-v_c)\,d^2C_{HL}/dz^2 = k_{LH}a_g\,(C_{HL}-C_{Hg}/K_H) \qquad (8)$$

Axial Dispersion in Liquid Phase — Diffusion from Gas-Liquid Interface to Liquid

$$+ k_H''C_{Fe}\,(1-v_c)\,(1-\epsilon_g)\,C_{HL}\,C_c/C_{ca}$$

Kinetic Dissipation at Catalyst Surface

with following boundary conditions:

$$C_{Hg} = C_{Hg}^{\,i} \qquad dC_{HL}/dz = 0 \text{ at } z = 0 \qquad (9a)$$

$$dC_{HL}/dz = 0 \text{ at } z = L \qquad (9b)$$

Catalyst Settling

$$E_c d^2C_c/dz^2 + u_{cs}\, dC_c/dz = 0 \qquad (10)$$

Catalyst Axial Dispersion — Catalyst Settling

$$E_c\, dC_c/dz + u_{cs}C_c = 0 \text{ at } z = 0 \text{ or } z = L \qquad (11a)$$

$$\int_0^L C_c(z)\, dz/L = C_{ca} \qquad (11b)$$

The non-mixed (NM) and perfectly mixed (PM) liquid models represent extremes of liquid mixing, while the axial dispersion (AD) model represents the liquid mixing predicted by correlations using axial dispersion coefficients from open literature. The NM model is similar to that used by Deckwer et al. (1981a), although Deckwer erroneously stated that the model represents perfect mixing in the liquid. The new model used here also accounts for the catalyst settling, while Deckwer et al. (1981a) neglected that effect. The AD model is similar to that described by Deckwer et al. (1982b), with simplifications of

no axial dispersion in the gas and isothermal operation.

The catalyst concentration along the bubble-column reactor can be obtained directly by solving equations (10)-(11), as:

$$C_c/C_{ca} = Pe_c(\exp(-Pe_c\bar{z}))/(1-\exp(-Pe_c)) \quad (12)$$

Assuming that the molar contraction due to the F-T reaction is linear with respect to the $H_2$+CO conversion, the following relation between the gas superficial velocity and the $H_2$+CO conversion was obtained:

$$u_g = u_g^{\,i}\,(1 + \alpha\, X_{H_2+CO}) \quad (13)$$

where $\alpha$ is the constant molar contraction factor.

Introducing equations (12) and (13) into equations (5)-(9) and then converting them to dimensionless form yields:

Gas Phase

$$((1+\alpha^*)/(1+\alpha^*\bar{y})^2)d\bar{y}/d\bar{z} = St_d\,(\bar{x}-\bar{y}) \quad (14)$$

Liquid Phase

NM Case:

$$St_d\,(\bar{y}-\bar{x}) = St_k\,C_c\,\bar{x} \quad (15)$$

PM Case:

$$\int_0^1 St_d\,(\bar{y}-\bar{x})\,dz = St_k\,\bar{x} \quad (16)$$

AD Case:

$$Pe_L^{-1}\,d^2\bar{x}/d\bar{z}^2 = K_H\,St_d\,(\bar{x}-\bar{y}) + K_H\,St_k\,C_c\,\bar{x} \quad (17)$$

with following boundary conditions:

$$\bar{y}=1 \qquad d\bar{x}/d\bar{z} = 0 \qquad \text{at } \bar{z} = 0 \quad (18a)$$

$$d\bar{x}/d\bar{z} = 0 \qquad \text{at } \bar{z} = 1 \quad (18b)$$

For the NM and PM cases, the equations can be solved analytically, giving the $H_2$ conversion as an implicit function of the parameters:

NM Case:

$$L= -u_g{}^i R_d(\alpha^* X_H{}^e+(1+\alpha^*)Ln(1-X_H{}^e))-E_c(Ln\ B_1)/u_{cs} \quad (19)$$

where:

$$B_1=(Pe_c+B_2(1-\exp(-Pe_c)))/(Pe_c-B_2(1-\exp(Pe_c))) \quad (20)$$

$$B_2=R_k/R_d \quad (21)$$

PM Case:

$$L= -u_g{}^i R_d(\alpha^* X_H{}^e+(1+\alpha^*Y)Ln(1-X_H{}^e/Y))/(1+\alpha^*Z) \quad (22)$$

where Y is defined as $(1-Z)/(1+\alpha^*Z)$ and $X_H$ ($H_2$ conversion) as $1-u_gC_{Hg}/u_g{}^iC_{Hg}{}^i$. By integration of Equation (5) and substitution of the resulting equation into Equation (7), a relation between Z and $X_H{}^e$ is established as follows:

$$Z = X_H{}^e/St_k \quad (23)$$

Substitution of Equation (23) into Y and Equation (22) gives the implicit relation between $X_H{}^e$ and L.

For the AD case, the model equations are non-linear, due to the variation of the gas superficial velocity with the molar contraction (term $(1+\alpha^*)/(1+\alpha^*\bar{y})^2$ in Equation (14)). A solution can be obtained by using an orthogonal collocation method (Villadsen and Michelsen, 1978).

Basically, the method uses a linear combination of one of the many families of orthogonal polynomials as a trial solution to the dependent variables. In the present application, the Jacobi polynomials with a weighting function $\bar{z}(1-\bar{z})$ are used. This family of polynomials is defined by the following equation:

$$P_j(\bar{z}) = \sum_{i=0}^{j} (-1)^{j-i}\ \gamma_{ij}\ \bar{z}^i \quad (24)$$

where

$$\gamma_{0j} = 1 \text{ for all } j \quad (25a)$$

$$\gamma_{ij} = \gamma_{i-1,j}\ (j-i+1)(j+i+2)/i(i+1) \quad (25b)$$

The orthogonality relation is given as

$$\int_0^1 \bar{z}\ (\bar{z}-1)\ P_i(\bar{z})\ P_j(\bar{z})\ d\bar{z} = 0 \quad \text{if } i = j \tag{26}$$

The trial solutions for both $\bar{x}$ and $\bar{y}$, truncated to Nth order polynomials as

$$\bar{x} = \sum_{i=0}^{N+1} a_i\ P_i(\bar{z}) \tag{27a}$$

$$\bar{y} = \sum_{i=0}^{N+1} a_{N+2+i}\ P_i(\bar{z}) \tag{27b}$$

are substituted into Equations (14) and (17), and boundary conditions (18a) and (18b). The collocation method dictates that the trial solutions satisfy these equations exactly at the N interior collocation points, which are the zeros of the Nth order polynomial, and at two boundaries. This results in 2(N+2) algebraic equations containing 2(N+2) unknowns. However, the resulting algebraic equations are nonlinear; therefore, an iterative scheme is used to solve these equations. In the current application, the Newton-Raphson routine is used. The criteria of the iteration scheme is that the successive dependent variables at all collocation points and the reactor exit are within 0.1% of each other. Another independent iterative scheme involves a convergence of the hydrogen concentration in the reactor exit, which is used to evaluate some parameters used in the model calculation. The criteria for this iteration is that its successive values are within 1% of each other. It was found that five collocation points were sufficient to give accurate results in most cases.

The correlations used to estimate the various model parameters are given in Table 27. All the parameters are defined in the Nomenclature.

2. Multi-Component Model

This improved model includes multi-component ($H_2$, CO, $CO_2$, and $H_2O$) mass transfer; water-gas shift reaction; and, non-linear kinetics. This model gives a more realistic understanding of the F-T slurry reactor performance which will be discussed in Section D. The major assumptions different from those of the single component model are:

- Mass transfer resistances to $H_2$, CO, $CO_2$, and $H_2O$ diffusion at the liquid side of the gas-liquid interface.

Table 27

Correlations Used In F-T Slurry Reactor
Mathematical Model Calculations

| Correlations[1] | References |
|---|---|
| $\rho_L = .758 - .555 \times 10^{-3}(T-373)$, g/cm$^3$ | Deckwer, et al. (1982b) |
| $\mu_L = .052 \exp(-6.905+3266/T)$, g/cm-s | Deckwer, et al. (1982b) |
| $D_{LH} = 7.35 \times 10^{-3} \exp(-2285/T)$, cm$^2$/s | Satterfield & Huff (1980) |
| $K_H = (2.291 \times 10^4 \exp(-1.2326+1583/T))/R_G T$ | Peter & Weinert (1955) |
| $\mu_{sl} = \mu_L(1 + 4.5\ v_c)$, g/cm-s | Deckwer, et al. (1982b) |
| $\epsilon_g = .053\ u_g^{1.1}$ | Deckwer, et al. (1982b) |
| $k_L = .31(\mu_{sl} g(\rho_{sl}-\rho_g)/\rho_{sl}^2)^{1/3}\ Sc^{-2/3}$, cm/s | Calderbank & Moo-Young (1961) |
| $Sh \geq 2$ | Saenger & Deckwer (1981) |
| $E_L = 3.676\ u_g^{.32}\ d_R^{1.34}$, cm$^2$/s | Shah & Deckwer (1982) |
| $E_c = u_g\ d_R\ (1+8\ Fr^{.85})/13\ Fr$, cm$^2$/s | Kato, et al. (1972) |
| $u_{cs} = 1.2\ u_{ct} \left\lvert \frac{u_g}{u_{ct}} \right\rvert^{.25} \left\lvert \frac{1-v_c}{1-v^*_c} \right\rvert^{2.5}$, cm/s | Kato, et al. (1972) |
| $Re = Ar/18$ | Kato, et al. (1972) |

[1] T in °K.

- Two consecutive reactions:

  - Fischer-Tropsch

$$CO + (1 + m/2)\ H_2 = (-CH_m) + H_2O \qquad (28)$$

$$r_1=k_1\ [H_2][CO]/([CO] + k_3[H_2O]) \qquad (29)$$

  - Water-Gas Shift

$$CO + H_2O = CO_2 + H_2 \qquad (30)$$

$$r_2=k_2\ ([CO][H_2O]-[H_2][CO_2]/k_4)/([CO]+k_3[H_2O]) \qquad (31)$$

- Gas holdup varies with the local gas-superficial velocity.

- Non-mixed liquid.

The rate expression for the Fischer-Tropsch reaction, Equation (29), follows the work by Dry (1976). In both the rate expressions (29) and (31), [ ] signifies volumetric concentrations. Note that the same denominator is used in both rate expressions. This is consistent with the hypothesis of competitive adsorption of active species on the same catalytic active sites (Langmuir-type adsorption isotherm, Satterfield, 1980). Only the [CO] and [$H_2O$] appearing in the denominator indicate that both are strongly absorbed on the catalyst active sites.

Material balances for the gas- and liquid-phase of the components $H_2$, CO, $CO_2$ and $H_2O$ (denoted by subscripts 1, 2, 3, 4, respectively), yield:

$$d(u_gC_{gi})/dz = -k_{Li}a_g(C_{gi}/K_i-C_{Li}),\ i = 1,\ldots,4 \qquad (32)$$

Convection in Gas Phase — Diffusion from Gas-Liquid Interface to Liquid

for the gas-phase, and

$$k_{Li}a_g(C_{gi}/K_i-C_{Li}) = -(1-\epsilon_g)(1-v_c)C_{Fe}\Sigma S_{ij}r_j,\ i = 1,\ldots,4 \qquad (33)$$

Diffusion from Gas-Liquid Interface to Liquid — Kinetic Dissipation at Catalyst Surface

for the liquid-phase, with the following inlet conditions:

$$C_{gi} = C_{gi}^{i} \text{ at } z = 0, \; i = 1,\ldots,4 \tag{34}$$

where $r_1$ and $r_2$ are, respectively, the F-T and the water-gas shift reaction rates given by Equations (29) and (31), and $S_{ij}$ ($i = 1,\ldots,4$; and $j = 1, 2$) are elements of the stoichiometric matrix.

The molar contraction resulting from the F-T reaction is the same as that used in the single component model (Equation (13)).

In dimensionless form, Equations (32) to (34) become:

$$d(\bar{u}_g \bar{C}_{gi})/d\bar{z} + St_{di}(\bar{C}_{gi} - \bar{C}_{Li}) = 0 \tag{35}$$

$$St_{di}(\bar{C}_{gi} - \bar{C}_{Li}) + \Sigma \, S_{ij} St_{kj} \bar{r}_j = 0 \tag{36}$$

$$\bar{C}_{gi} = \bar{C}_{gi}^{i} \text{ at } \bar{z} = 1 \tag{37}$$

for $i = 1,\ldots,4$.

A solution for this set of non-linear equations can be obtained using the orthogonal collocation method (Villadsen and Michelsen, 1978). This method dictates that the trial solutions (linear combinations of orthogonal polynomials described in Subsection VII.C.1), satisfy the gas-phase and the liquid-phase equations exactly at the N interior collocation points, the inlet point, and the exit point. This results in a system of 8N+12 non-linear algebraic equations, which are solved simultaneously by a Newton-Raphson routine. The convergence criterion of the iterative scheme is that the successive dependent variables at all collocation points be within 0.1% of each other. It was found that five collocation points were sufficient in most calculations as shown in Figure 36. The correlations used to calculate the parameters are summarized in Table 28. Those correlations that are common to both simple-component and multi-component models are given in Table 27.

Note that using variable gas holdup and interfacial area along the reactor length gives virtually identical results as the case of an average gas holdup and interfacial area as discussed later (see Subsection VIII.D.2.b). In the current case, the use of variable gas holdup and interfacial area actually simplifies the numerical iteration scheme, avoiding the necessity of an additional iteration on the parameters $St_{kj}$ and $St_{di}$ (which are dependent on $\epsilon_g$ and $a_g$).

FIGURE 36

EFFECT OF NUMBER OF COLLOCATION POINTS ON THE PREDICTED F-T BUBBLE-COLUMN PERFORMANCE (Base Case)

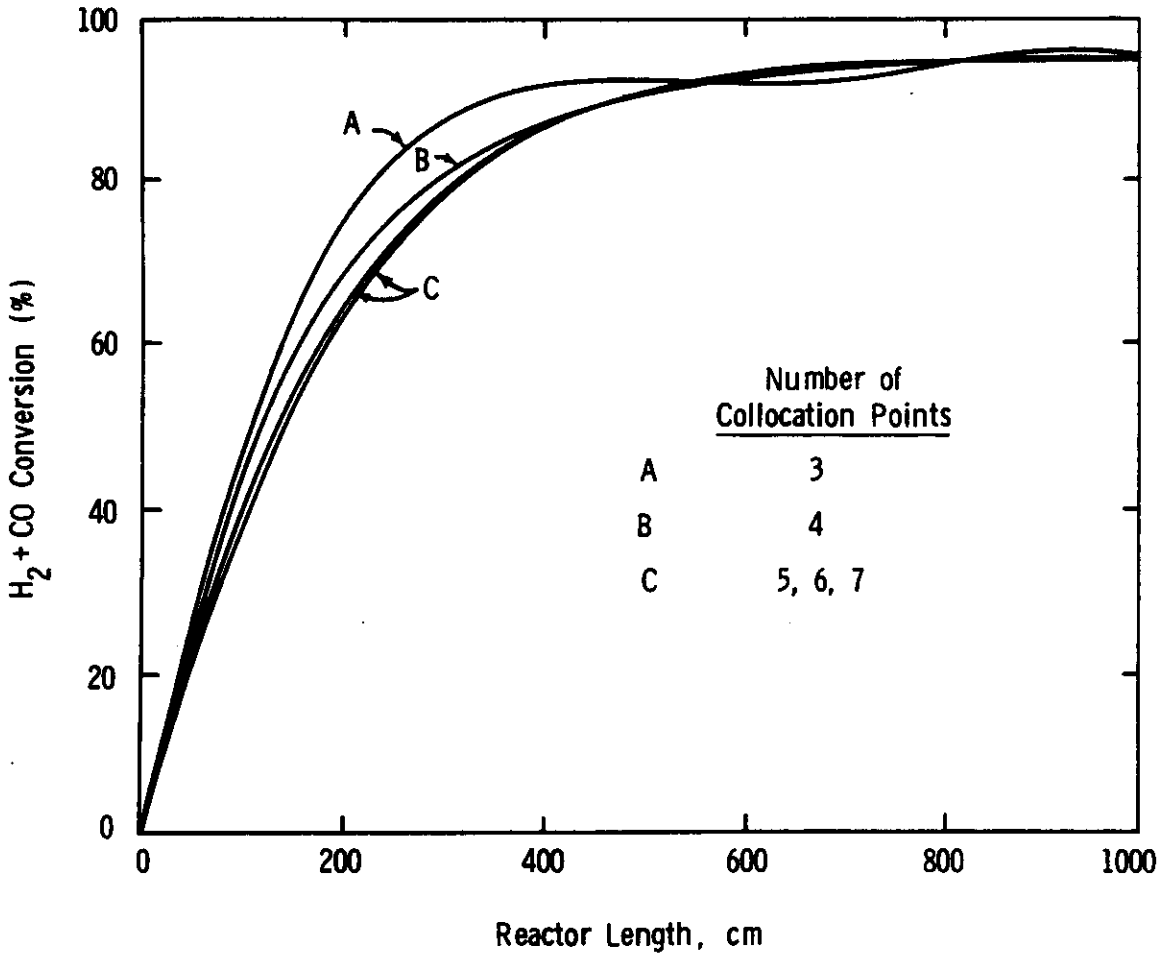

## Table 28

## Correlations for Solubility and Diffusivity[1]

| | | |
|---|---|---|
| **Solubility ($cm^3$ liquid/$cm^3$ gas)** | | |
| $H_2$ $746\ T^{-1}exp\ (639.9/T)$ | Experimental | Koelbel, et al. (1955)<br>Peter & Weinert (1955) |
| CO $878\ T^{-1}exp\ (440.2/T)$ | " | " |
| $CO_2$ $2970\ T^{-1}exp\ (-608.4/T)$ | " | " |
| $H_2O$ $6740\ T^{-1}exp\ (-1270/T)$ | " | " |
| **Diffusivity ($cm^2/s$)** | | |
| $H_2$ $3.90 \times 10^{-2}exp\ (-2877/T)$ | Experimental + Correlation[2] | Peter & Weinert (1956) |
| CO $5.99 \times 10^{-4}exp\ (-1633/T)$ | Experimental + Correlation[3] | Zaidi, et al. (1979) |
| $CO_2$ $3.70 \times 10^{-4}exp\ (-1437/T)$ | Experimental + Correlation[2] | Hayduk & Cheng (1971) |
| $H_2O$ $9.6 \times 10^{-4}exp\ (-1633/T)$ | Experimental + Correlation | Hayduk & Cheng (1971) |

[1] T in °K.

[2] Extrapolation using correlation of diffusivity with liquid viscosity.

[3] Estimates of $D_{\ell 2}$ from correlation produced mass transfer coefficients which fitted experimental data.